論文内容の要旨

論文題目：

Relationship between anatomical and functional connectivity in the macaque cerebral cortex: an fMRI study

（マカクサル大脳皮質における解剖学的結合と機能的結合の関係：核磁気共鳴機能画像法による研究）

氏名：　　足立　雄哉

Functional connectivity (FC) in the cerebral cortex of humans in the resting state and of anesthetized macaque monkeys measured by functional magnetic resonance imaging (fMRI) is commonly assumed to reflect the underlying anatomical connectivity (AC). But it is known that cortical regions with no direct anatomical connection can also have strong FC, suggesting an important role of indirect anatomical pathways mediated by multiple cortical regions on the shaping of FC. The direction of axonal projections along the pathways essentially determines the causal directions in the neuronal interactions; nevertheless, there has been no empirical study on how the directionality of AC contributes to FC at the inter-areal level, because of the lack of noninvasive techniques to distinguish the directionality of AC in humans.

In macaque monkeys, anatomical projections across a wide range of brain regions have been investigated for decades, and their directionality is known. In this study, by using fMRI in macaque monkeys, we examined empirically how FC between an area pair is dependent on indirect AC patterns between the pair, and we investigated computationally how this relationship depends on the global network structure of the cerebral cortex.

We acquired BOLD fMRI in anesthetized macaque monkeys with a 4.7-T MRI scanner and extracted the time series of BOLD signals from 39 regions in each hemisphere of the animals. Then, by correlating the BOLD time series after preprocessings, FC was computed in all the area pairs within each hemisphere in each BOLD run. Figure 1a shows the FC matrix averaged across all BOLD runs and across both hemispheres from all animals. Information about the presence and the

direction of anatomical connections among the macaque cortical areas examined in the present study (Fig. 1b) is based on the CoCoMac database of past tracer studies in the macaque monkeys.

In the empirical FC and AC matrices (Figs 1a and 1b), area pairs with direct AC (unidirectional or bidirectional) indeed have larger FC on average than those with no direct AC, but considerable proportions of unconnected area pairs have FC values comparable to connected area pairs (Fig. 1c). We examined how the number of indirect anatomical connections between an area pair affects the FC of the area pair. In the macaque FC (Fig. 1a) and AC (Fig. 1b) matrices, FC of area pairs with no direct AC significantly increases with the total number of the indirect AC mediated by just one area in-between ('length-2 AC') (linear regression, n = 479, slope = 6.6×10^{-3}, $P < 0.001$). However, the number of indirect AC with two areas in-between ('length-3 AC') does not contribute to the increase of FC in area pairs with neither direct nor length-2 AC (linear regression, n = 74, slope = -7.3×10^{-4}, $P = 0.03$). In the macaque AC matrix (Fig. 1b) there is only one area pair with neither direct, length-2, nor -3 AC, and there is no area pair with neither direct, length-2, -3, nor -4 AC. These results imply that FC increases with the number of indirect AC only at length-2 AC.

The information about the directionality of tract projections in the macaque monkey allowed us to distinguish the six different length-2 AC patterns (A to F in Fig. 2a), which are not distinguishable in diffusion MRI tractography. Then we examined whether these six length-2 AC patterns make differential contributions to FC in the macaque monkey. The contribution of each length-2 AC pattern to FC (Fig. 2a) was estimated for each hemisphere of each monkey by using multiple linear regressions ($P < 0.001$ in the fittings for all the hemispheres). A three-way ANOVA for the estimated contributions (AC pattern × Monkey × Hemisphere) revealed a significant main effect of AC pattern ($F_{5,5} = 8.18$, $P < 0.05$), no significant main effects of Monkey and Hemisphere ($F_{1,5} = 0.57$ and $F_{1,5} = 0.89$ respectively, $P > 0.1$ for both), and no significant two-way interactions ($P > 0.05$ for all). In particular we focused on the comparison of the directed AC patterns (motifs) of 'common efferents'

Figure 1

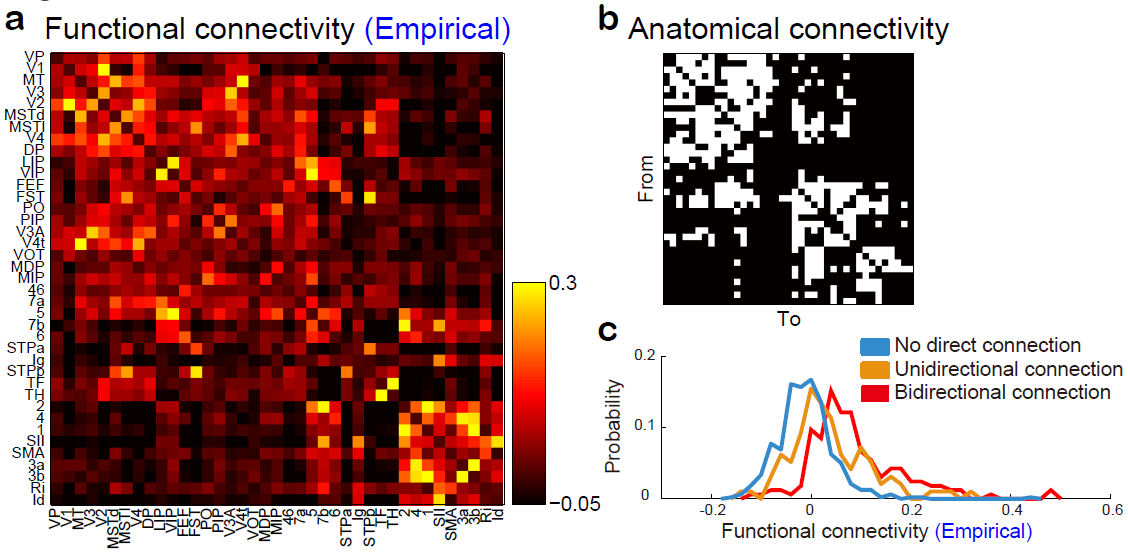

(pattern A), 'disynaptic relay' (pattern B), and 'common afferents' (pattern C). Based on the apparent causal relationships represented in the AC patterns A, B, and C, one might expect that the contribution of common efferents (pattern A) to FC is smaller than that of the other two patterns; however, our comparison revealed that, contrary to the expectation, not only common afferents (pattern C) but also common efferents (pattern A) make greater contributions to FC than the disynaptic relay (pattern B) ($P < 0.01$, Tukey test).

This counterintuitive observation demands an interpretation from a viewpoint beyond the local aspects of the AC patterns. Therefore we computationally investigated how the global network structure relates to this empirical observation. A previous computational study (Honey et al. 2007) simulated BOLD time series of macaque cortical areas including the areas examined in the present empirical data, based on a model incorporating empirically known axonal projections ('macaque-type anatomical network'). The FC matrix based on the simulated BOLD time series ('macaque-type simulation') significantly correlates with the empirical FC (Fig. 1a) ($R = 0.55$, $P < 0.001$). We confirmed that the above-mentioned relations between FC and AC in the empirical data are preserved in the macaque-type simulation: the significant difference of FC between area pairs with direct AC (bidirectional and unidirectional) and those with no direct AC and the significant positive contribution of the combined length-2 AC to FC (linear regression, slope = 1.0×10^{-2}, $P < 0.001$). Most importantly, the respective contributions of the length-2 AC patterns are also preserved (correlation coefficient $R = 0.91$, $P < 0.05$; Fig. 2b). We defined the z-score-transformed correlation coefficient as the 'match-with-empirical index' (MEI; MEI = 2.64 for the macaque-type simulation). MEI represents how well the simulation preserves the contributions of the length-2 AC patterns. These agreements strongly suggest that the empirically detected contributions of length-2 AC patterns to FC (Fig. 2a) are induced by the anatomical network that is shared by the macaque-type simulation and the real macaque neocortex.

Figure 2

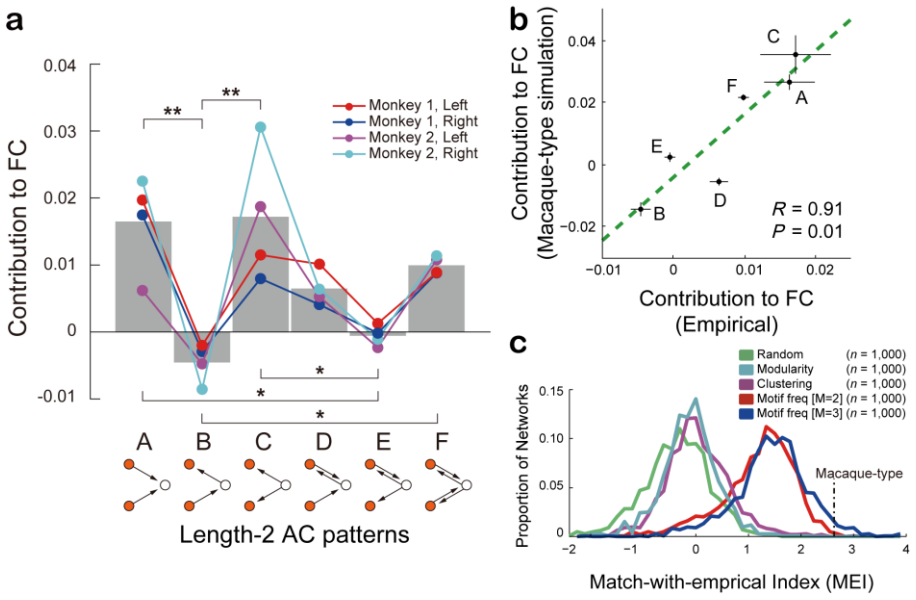

Thus, we can computationally investigate whether the contributions of the length-2 AC patterns to FC (Figs. 2a and 2b) are specific to the macaque cortical network, by comparing the MEI in the macaque-type simulation with the MEIs in simulations on randomly rewired anatomical networks. We first generated random anatomical networks in which the number of afferent and efferent connections of each area (degree) is matched with that in the macaque-type network. Then we simulated the BOLD-FC matrix and computed the MEI for each random network. Compared with all the random networks (n = 1,000), the MEI of the macaque-type network is exceptionally large (P < 0.001; Fig 2c). Therefore the empirically detected contributions of length-2 AC patterns to FC (Fig. 2a) are unique to the anatomical network of the macaque cortex.

Next we examined whether some network metrics can capture the uniqueness of the macaque cortical network that appears in the local AC-FC relation. As the candidates for the metrics, we focused on the clustering coefficient, the modularity, and the motif frequencies of size M = 2 and 3 (mf2 and mf3). The clustering coefficient and the modularity are found at higher levels in the macaque network. For each metric we constructed rewired anatomical networks (n = 1,000) in which the values of the metric as well as the degrees are matched with those of the macaque-type network. Then, for each network, the BOLD-FC matrix was simulated, and the MEI was computed. Figure 2c shows that the mf2-matched (MF2) and the mf3-matched (MF3) networks have significantly larger MEIs than other networks (P < 0.001). These results suggest that the configuration of anatomical motifs in the cortical network have a role in generating the contributions of length-2 AC patterns that are empirically observed. Nonetheless, in all of the four sets of metric-matched networks, the MEI of the macaque-type network is highly exceptional (P < 0.001, P = 0.002, P = 0.04, and P = 0.037 for MD, CL, MF2, and MF3 networks, respectively; Fig. 2c). Thus these network metrics might not fully capture the unique properties of the macaque cortical network.

Our results demonstrate how macaque cortical FC is dependent on local AC patterns and on the direction of inter-regional pathways (Fig. 2a). The AC-FC relation is not determined solely by local inter-regional causality but instead is dominated by the network-level anatomical architecture of the cortex (Fig. 2c), which would include the distribution and arrangement of directed anatomical motifs and the hierarchical organization of the cerebral cortex. The observation that the contributions of common efferents and afferents to FC are larger than that of the disynaptic serial relay supports the notion that functionally related areas have common profiles of anatomical inputs and outputs. The high consistency of empirical and simulated FC also suggests that the local AC-FC relations revealed in this study are largely supported by cortico-cortical pathways, and less dependent on anatomical links with subcortical structures.